BIOCHEMISTRY
including biophysical chemistry & molecular biology

Article

pubs.acs.org/biochemistry

Activity Enhancement of the Synthetic Syrbactin Proteasome Inhibitor Hybrid and Biological Evaluation in Tumor Cells

Crystal R. Archer,[‡,§,#] Michael Groll,[∥] Martin L. Stein,[∥] Barbara Schellenberg,[⊥,●] Jérôme Clerc,[@,○] Markus Kaiser,[@] Tamara P. Kondratyuk,[†] John M. Pezzuto,[†,§] Robert Dudler,[⊥] and André S. Bachmann*[,†,‡,§]

[†]Department of Pharmaceutical Sciences, College of Pharmacy, University of Hawaii at Hilo, 34 Rainbow Drive, Hilo, Hawaii 96720, United States

[‡]University of Hawaii Cancer Center, 1236 Lauhala Street, University of Hawaii at Manoa, Honolulu, Hawaii 96813, United States

[§]Department of Cell and Molecular Biology, John A. Burns School of Medicine, University of Hawaii at Manoa, 651 Ilalo Street, Honolulu, Hawaii 96813, United States

[∥]Center for Integrated Protein Science at the Department Chemie, Technische Universität München, Lichtenbergstrasse 4, 85747 Garching, Germany

[⊥]Zürich-Basel Plant Science Center, Institute of Plant Biology, University of Zürich, Zollikerstrasse 107, 8008 Zürich, Switzerland

[@]Zentrum für Medizinische Biotechnologie, Fakultät Biologie & Fakultät für Chemie, Universität Duisburg-Essen, Universitätsstrasse 2, 45141 Essen, Germany

Supporting Information

ABSTRACT: Syrbactins belong to a recently emergent class of bacterial natural product inhibitors that irreversibly inhibit the proteasome of eukaryotes by a novel mechanism. The total syntheses of the syrbactin molecules syringolin A, syringolin B, and glidobactin A have been achieved, which allowed the preparation of syrbactin-inspired derivatives, such as the syringolin A–glidobactin A hybrid molecule (SylA–GlbA). To determine the potency of SylA–GlbA, we employed both in vitro and cell culture-based proteasome assays that measure the subcatalytic chymotrypsin-like (CT-L), trypsin-like (T-L), and caspase-like (C-L) activities. We further studied the inhibitory effects of SylA–GlbA on tumor cell growth using a panel of multiple myeloma, neuroblastoma, and ovarian cancer cell lines and showed that SylA–GlbA strongly blocks the activity of NF-κB. To gain more insights into the structure–activity relationship, we cocrystallized SylA–GlbA in complex with the proteasome and determined the X-ray structure. The electron density map displays covalent binding of the Thr1O$^{\gamma}$ atoms of all active sites to the macrolactam ring of the ligand via ether bond formation, thus providing insights into the structure–activity relationship for the improved affinity of SylA–GlbA for the CT-L activity compared to those of the natural compounds SylA and GlbA. Our study revealed that the novel synthetic syrbactin compound represents one of the most potent proteasome inhibitors analyzed to date and therefore exhibits promising properties for improved drug development as an anticancer therapeutic.

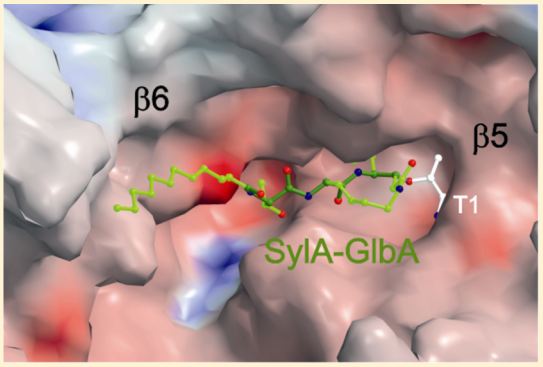

Syrbactins are natural product small molecules that include the syringolins and glidobactins. While syringolins were identified more recently in isolates from the plant pathogen *Pseudomonas syringae* pv *syringae* (*Pss*),[1] the structurally related glidobactins were discovered in the 1980s from an unknown species of the order Burkholderiales.[2−5] Syringolin A (SylA) and glidobactin A (GlbA) represent the predominant forms in these bacterial pathogens, whereas SylB-F and GlbB-F are naturally occurring syrbactin variants expressed in minor quantities.[1,6,7]

In 2006, we demonstrated that the plant pathogen-derived natural product SylA induces massive p53 accumulation followed by apoptosis in neuroblastoma and ovarian tumor cells.[8] Two years later, we discovered that SylA represents a bacterial virulence factor that irreversibly inhibits the eukaryotic proteasome by a novel mechanism.[9] The proteasome is a multiprotein complex that is responsible for intracellular protein degradation, both via ubiquitin-dependent and via ubiquitin-independent proteolysis.[10−13] Many of these proteasome-controlled proteins regulate cell division, proliferation, and apoptosis, and proteasome inhibitors represent a promising family of antineoplastic agents.[12−19] Bortezomib (Velcade) is the first proteasome inhibitor approved by the U.S. Food and

Received: June 22, 2012
Revised: August 4, 2012
Published: August 7, 2012

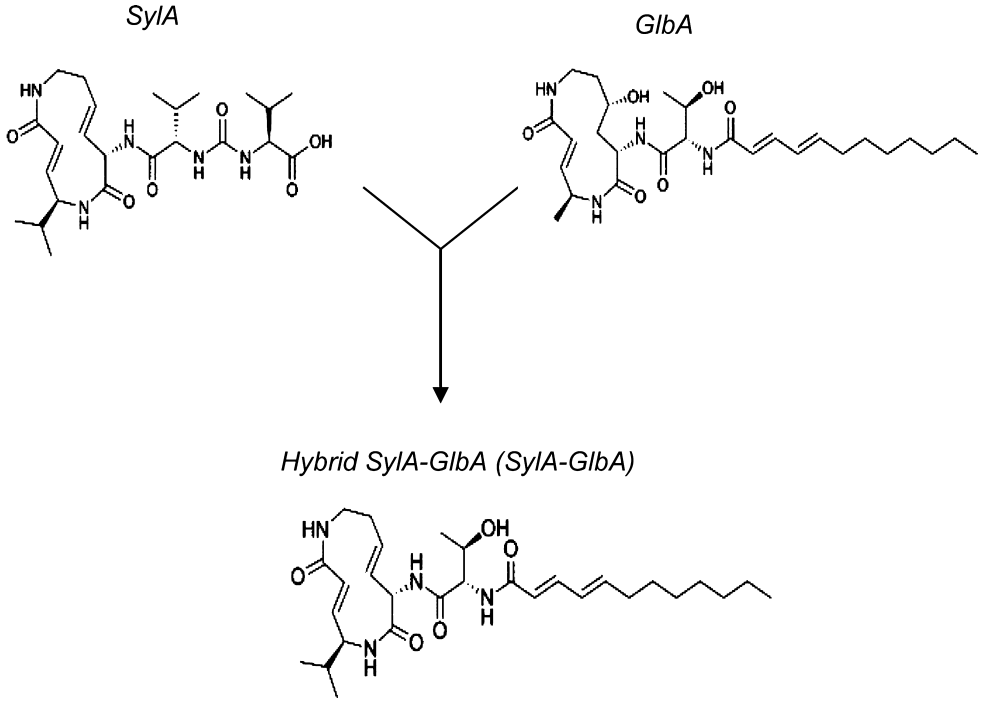

Figure 1. Chemical structures of SylA, GlbA, and the SylA−GlbA hybrid molecule. (A) Syringolin A (SylA) is a natural product produced by the plant pathogen *P. syringae* pv *syringae* (*Pss*) and acts as a moderately potent proteasome inhibitor. (B) Glidobactin A (GlbA) is a natural product proteasome inhibitor produced by an unknown species of the order Burkholderiales that is termed strain K481-B101 (ATCC 53080). (C) SylA−GlbA is a synthetic hybrid of SylA and GlbA.

Drug Administration (FDA) for the treatment of refractory and/or relapsed multiple myeloma (MM) and mantle cell lymphoma, and preclinical studies have validated a number of next-generation proteasome inhibitors such as carfilzomib (PR-171), marizomib (NPI-0052), and MLN9708.[13]

Despite its success on the market, bortezomib therapy has several disadvantages, including intravenous administration and multiple side effects such as thrombocytopenia, neutropenia, and gastrointestinal disorders. Bortezomib also leads to severe but reversible neurodegenerative effects and triggers nerve degeneration by exhibiting substantial off-target activity.[12] Additional challenges are the increasing chemoresistance and patient relapse in response to proteasome inhibitors, and one novel approach may be to target the immunoproteasome, a proteasomal variant found predominantly in cells of hematopoietic origin that differs from the constitutive proteasome found in most other cell types.[20] Indeed, the recent elucidation of the immune and constitutive proteasome crystal structures revealed important differences in substrate and inhibitor specificity,[21] thus providing new insights into the structure-guided design of novel lead structures that are selective for the immunoproteasome and subcatalytic proteasome activities.

We previously showed that SylA inhibits the chymotrypsin-like (CT-L), trypsin-like (T-L), and caspase-like (C-L) subcatalytic activities of the proteasome, while GlbA inhibits the CT-L and T-L but not C-L subcatalytic activities.[9] In 2009, the chemical synthesis of syringolin A and syringolin B was achieved,[22] which spurred the subsequent synthesis of novel syringolin- and glidobactin-inspired syrbactin analogues.[23−27] Of those, SylA-LIP and TIR-203 represent two novel analogues with improved biological activities.[24,27] Most recently, we synthesized the hybrid molecule SylA−GlbA (Figure 1) that consists of a SylA macrocycle connected to the lipophilic GlbA side chain and demonstrated that the SylA or GlbA macrocycle moiety has a critical influence on the β1 (C-L) subsite selectivity.[28] To further evaluate the potency of this novel syrbactin analogue, we performed a biological characterization of SylA−GlbA and determined the complex structure of the ligand with the proteasome to gain additional insights into inherent structure−activity relationships.

EXPERIMENTAL PROCEDURES

Synthesis and Natural Product Isolation of Syrbactins. The SylA−GlbA hybrid (SylA−GlbA) and synthetic SylA were synthesized as previously reported.[22,28,29] GlbA was isolated from its biological source as described previously.[1,30,31] All compounds were dissolved in sterile DMSO and frozen in aliquots at −20 °C. At the beginning of each experiment, aliquots were thawed and diluted to the final concentration.

Mammalian Cell Cultures and Reagents. The following panel of chemosensitive and chemoresistant cancer cell lines was used in this study. Human neuroblastoma (NB) cell line SK-N-SH was obtained from the American Type Culture Collection (ATCC).[32] Multiple myeloma (MM) cell lines MM1.S and MM1.RL are sensitive and resistant to dexamethasone, respectively. U266 is an IL-6-producing cell line isolated from the peripheral blood of a male myeloma patient. All myeloma cells were provided by N. Krett (Northwestern University, Evanston, IL).[33] Human ovarian cancer cell line SKOV3, which is resistant to several cytotoxic drugs, was available at the University of Hawaii Cancer Center.[34,35] Cells were seeded 18−24 h before syrbactin or bortezomib treatments and analyzed after 24−72 h. The human embryonic kidney 293/NF-κB-Luc cell line was designed for monitoring the activity of NF-κB and was purchased from Panomics (Freemont, CA). This cell line contains chromosomal integration of a luciferase reporter construct regulated by the NF-κB response element. Transcription factors can bind to the

dx.doi.org/10.1021/bi300841r | *Biochemistry* 2012, 51, 6880−6888

response element when stimulated by certain agents, allowing transcription of the luciferase gene. *N*-Tosyl-L-phenylalanyl chloromethyl ketone (TPCK) was purchased from Santa Cruz Biotechnology, Inc. (Santa Cruz, CA). (*E*)-3-(4-Methylphenylsulfonyl)-2-propenenenitrile (BAY-11) was purchased from Cayman Chemical (Ann Arbor, MI). Bortezomib was purchased from LC Laboratories (Woburn, MA).

In Vitro Proteasome Activity Assay. In vitro proteasome inhibition assays were performed in 96-well microtiter plates with human erythrocyte 20S proteasomes using the AK-740 Assay Kit for Drug Discovery (Biomol). Reactions were performed at 37 °C in 100 μL volumes containing a serial dilution of SylA−GlbA, 2 μg/mL 20S proteasome, and 100 μM Suc-LLVY-AMC, Boc-LRR-AMC, or Z-LLE-AMC for assaying CT-L, T-L, and C-L activities, respectively, according to the manufacturer's instructions. Fluorescence was monitored with an MWGt Sirius HT plate reader (BioTek Instruments, Luzern, Switzerland) equipped with 360 nm excitation and 460 nm emission filters.

In Vivo Proteasome Activity Assay. The cell culture-based in vivo proteasome-Glo activity assay was performed as previously described.[9,24] Clear-bottom, white-walled 96-well microtiter cell culture plates (Greiner Bio-One North America Inc., Monroe, NC) were seeded with cells as indicated and treated with syrbactin or bortezomib. Proteasome inhibition was measured using the proteasome Glo reagent according to the manufacturer's instructions (Promega, Madison, WI). In brief, tumor cells were treated with SylA−GlbA, SylA, GlbA, or bortezomib at different concentrations as indicated and incubated for 2 h. After incubation, cells were incubated for 15 min with 100 μL of proteasome Glo reagent, which permeabilizes cells and contains the bioluminescent substrates Suc-LLVY-aminoluciferin, Z-nLPnLD-aminoluciferin, and Z-LRR-aminoluciferin to determine the CT-L, T-L, and C-L activities, respectively. The luminescence was measured with a Dynex MLX luminometer.

Cell Proliferation Assay. The CellTiter 96 Aqueous One solution Cell Proliferation Assay [2-(4,5-dimethylthiazol-2-yl)-5-(3-carboxymethoxyphenyl)-2-(4-sulfophenyl)-2*H*-tetrazolium, inner salt (MTS)] (Promega, San Luis Obispo, CA) measures metabolic cell activity and was used to indirectly determine the viability of cells after treatment with SylA−GlbA for 48 h at the indicated concentrations (0−1 μM) by measuring the absorbance at 492 nm using a Perkin-Elmer HTS7000 Plus bioassay reader. The mean IC_{50} values in Table 1 were determined by setting the lowest dose at 100% and fitting normalized data to 3PL curve fitting in Prism from GraphPad Software, Inc. (La Jolla, CA).

NF-κB Activity Assay. The NF-κB activity assay was performed as previously described.[36] Briefly, HEK293/NF-κB-Luc cells were seeded into sterile white-walled 96-well plates at a density of 2×10^4 cells/well in Dulbecco's modified medium with 10% FBS. After cells had been grown for 48 h to 90% confluence, the medium was replaced with fresh medium containing tumor necrosis factor α (TNF-α) (final concentration of 30 ng/mL), and cells were treated simultaneously for 6 h with inhibitor compounds (SylA−GlbA, SylA, and GlbA) at various concentrations. To avoid false-positive responses, a cytotoxicity control experiment was included in parallel to ensure that the NF-κB activity changes within the 6 h incubation period are not due to cell death (data not shown). Luciferase activity was determined with a luciferase kit from Promega according to the manufacturer's instructions. Following treatment, the cells were washed with phosphate-buffered saline and 50 μL of 1× Reporter lysis buffer was added before plates were placed in a −80 °C freezer. The following day, the cells were thawed and assayed for luciferase activity with a LUMIstar Galaxy Luminometer (BMG Labtechnologies, Durham, NC). As a positive control, two NF-κB inhibitors were used: *N*-tosyl-L-phenylalanyl chloromethyl ketone (TPCK) and (*E*)-3-(4-methylphenylsulfonyl)-2-propenenenitrile (BAY-11). Results were expressed as a percentage relative to control (TNF-α-treated) samples, and dose−response curves were constructed for the determination of IC_{50} values, which were generated from the results of eight serial dilutions of inhibitor compounds. Data represent the mean of two independent experiments, each performed in triplicate ($n = 6$).

Table 1. Hybrid SylA−GlbA Inhibits the Proliferation of Tumor Cells

	IC_{50} values (nM)[a]
cell line	hybrid SylA−GlbA
MM1.S	28 ± 5
MM1.RL	27 ± 5
U266	45 ± 3
SKOV3	109 ± 64
SK-N-SH	321 ± 93

[a] IC_{50} is the inhibitory concentration at which cell viability is reduced by 50%. The mean IC_{50} values were determined by setting the lowest dose at 100% and fitting normalized data to 3PL curve fitting in Prism from GraphPad Software, Inc. (La Jolla, CA, USA). Data present the mean values of three independent experiments, each performed in triplicate wells ($n = 9$), ± SEM.

Cocrystallization. Crystals of the 20S proteasome from *Saccharomyces cerevisiae* were grown in hanging drops at 20 °C as previously described[37] and incubated for 48 h with SylA−GlbA at 10 mM. The protein concentration used for crystallization was 45 mg/mL in Tris-HCl (10 mM, pH 7.5) and EDTA (1 mM). The drops contained 1 μL of protein and 1 μL of the reservoir solution, containing 20 mM magnesium acetate, 100 mM morpholinoethanesulfonic acid (pH 6.9), and 10% MPD.

The compound belongs to space group $P2_1$ with the following cell dimensions: $a = 135.9$ Å, $b = 298.8$ Å, $c = 145.3$ Å, and $\beta = 112.6°$ (see Table S1 of the Supporting Information). Data to 2.8 Å for the proteasome−inhibitor complex were collected using synchrotron radiation with $\lambda = 1.0$ Å at beamline X06SA in SLS (Villingen, Switzerland). Crystals were soaked in a cryoprotecting buffer [30% MPD, 20 mM magnesium acetate, and 100 mM morpholinoethanesulfonic acid (pH 6.9)] and frozen in a stream of liquid nitrogen gas at 100 K (Oxford Cryo Systems). X-ray intensities were evaluated using XDS.[38] The anisotropy of diffraction was corrected by an overall anisotropic temperature factor by comparing observed and calculated structure amplitudes using CNS.[39,40] The electron density map was improved by averaging and back transforming the reflections 10 times over the 2-fold noncrystallographic symmetry axis using MAIN.[41] Conventional crystallographic rigid body, positional, and temperature factor refinements were conducted with CNS using the yeast 20S proteasome structure as a starting model.[42] Modeling experiments were performed with MAIN. Apart from the bound inhibitor molecules, structural changes were noted only in the specificity pockets. Temperature factor refinement indicates full occupancies of all inhibitor binding sites. The

dx.doi.org/10.1021/bi300841r | *Biochemistry* 2012, 51, 6880−6888

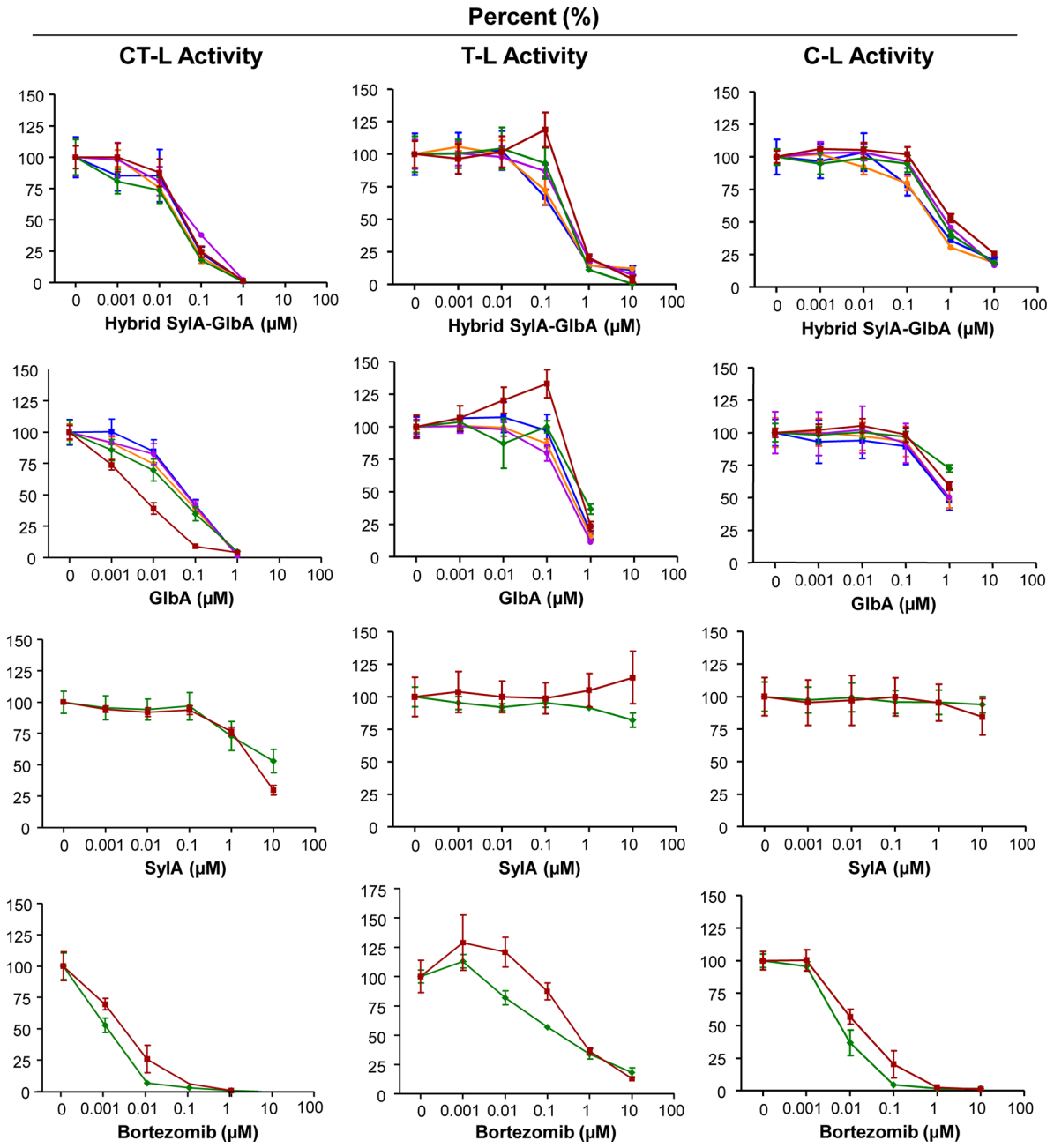

Figure 2. SylA−GlbA inhibits proteasomal activities of tumor cells in vivo. A panel of human tumor cell lines, including human multiple myeloma cell lines MM1.S (blue circles), MM1.RL (orange squares), and U266 (purple circles), human ovarian cancer cell line SKOV3 (green diamonds), and human neuroblastoma cell line SK-N-SH (red squares), were treated individually over a period of 2 h with SylA−GlbA at various drug concentrations (0−10 μM). The natural product wild-type SylA and the FDA-approved proteasome inhibitor bortezomib (Velcade) were included as controls and tested in two cell lines [SK-N-SH (red squares) and SKOV3 (green diamonds)]. The inhibition of the chymotrypsin-like (CT-L), trypsin-like (T-L), and caspase-like (C-L) proteasome activity was determined by incubating treated cells with the bioluminescent substrates Suc-LLVY-aminoluciferin, Z-LRR-aminoluciferin, and Z-nLPnLD-aminoluciferin to measure the CT-L, T-L, and C-L proteasome activities, respectively. Data normalized to controls represent the mean of three independent experiments, and each experiment was performed in duplicate (n = 6); bars show the standard deviation. The CT-L activity measurements for GlbA, SylA, and bortezomib have been previously reported.[24]

inhibitors have been omitted for phasing. The refined proteasome:SylA−GlbA complex structures revealed current crystallographic values for R_{cryst} of 0.212 and for R_{free} of 0.237[43] (Table S1 of the Supporting Information).

RESULTS

SylA−GlbA Inhibits All Three Catalytic Activities of the Proteasome. In an effort to generate more effective SylA analogues that exhibit higher potency, we recently synthesized a hybrid molecule that combines SylA with properties of GlbA.[28] As shown in Figure 1, the hybrid molecule SylA−GlbA is built up from the SylA macrocycle connected to the GlbA side chain. To determine the resulting inhibitory properties of this hybrid molecule, we employed an in vitro proteasome assay. In this assay, SylA−GlbA inhibited the CT-L activity with an apparent K_i of 12.5 ± 1.5 nM, the T-L activity with an apparent K_i of 136.9 ± 12.4 nM, and the C-L activity with an apparent K_i of 3.7 ± 1.2 μM, thereby demonstrating that the proteasome

dx.doi.org/10.1021/bi300841r | Biochemistry 2012, 51, 6880−6888

inhibitor SylA−GlbA is one of the most potent syrbactins reported to date.

To corroborate the in vitro analysis, we tested the effectiveness of SylA−GlbA in a cell culture-based system that allows the detection of each subcatalytic proteasome activity in vivo. As shown in Figure 2, SylA−GlbA inhibited the CT-L, T-L, and C-L activities in a dose-dependent manner, in five cancer cell lines representing multiple myeloma (MM1.S, MM1.RL, and U266), neuroblastoma (SK-N-SH), and ovarian cancer (SKOV3). The syrbactin GlbA inhibited the proteasomal activities in a similar fashion. SylA and bortezomib were included as controls and tested in two cell lines (SK-N-SH and SKOV3). While SylA showed an expected weaker response with the strongest inhibitory effects against the CT-L activity of the proteasome, the FDA-approved proteasome inhibitor bortezomib (Velcade) strongly inhibited the three catalytic activities in these two cell lines, with the highest potency against the CT-L activity.

SylA−GlbA Inhibits the Proliferation of Tumor Cells More Effectively Than SylA. To examine the effect of SylA−GlbA-induced proteasome inhibition on cancer cell proliferation, we tested five cancer cell lines in the presence of increasing inhibitor concentrations (Figure 3). The inhibitory

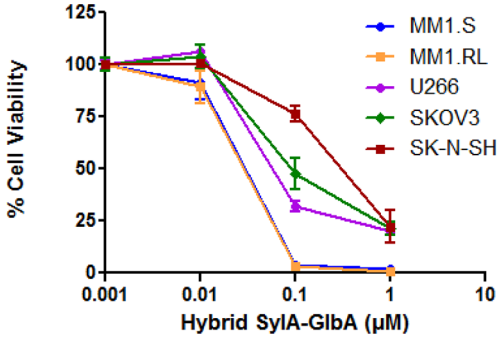

Figure 3. SylA−GlbA inhibits the proliferation of tumor cells. A panel of human tumor cell lines, including human multiple myeloma cell lines MM1.S (blue circles), MM1.RL (orange squares), and U266 (purple circles), human ovarian cancer cell line SKOV3 (green diamonds), and human neuroblastoma cell line SK-N-SH (red squares), were treated individually over a period of 48 h with SylA−GlbA at various concentrations (0−1 μM). The viability of cells was determined by the MTS assay. Data normalized to controls represent the means of three independent experiments, and each experiment was performed in triplicate (n = 9); bars show the standard error of the mean.

effect of SylA−GlbA was most prominent in multiple myeloma MM1.S cells and equally potent in dexamethasone-resistant multiple myeloma MM1.RL cells. SylA−GlbA also decreased the cell viability of multiple myeloma U266 cells, ovarian cancer SKOV3 cells, and neuroblastoma SK-N-SH cells in a dose-dependent fashion. At concentrations of ≥0.1 μM, cell growth inhibition was 100% in both multiple myeloma cell lines MM1.S and MM1.RL. The concentration at which cell growth is inhibited by 50% (IC_{50}) was calculated (Table 1) and determined at 28 nM (MM1.S), 27 nM (MM1.RL), 45 nM (U266), 109 nM (SKOV3), and 321 nM (SK-N-SH). In contrast, the IC_{50} values previously reported for SylA are between 9 and 39 μM (depending on the cancer cell line),[8,24] thus confirming that the novel hybrid syrbactin SylA−GlbA exhibits significantly more potent (100−2000-fold) antiproliferative activity than SylA.

Syrbactins Inactivate TNF-α-Induced NF-κB Activity. To determine whether NF-κB inactivation might be the underlying mechanism of proteasome inhibitor-induced cell death, three syrbactins (SylA−GlbA, SylA, and GlbA) were tested in a cell culture-based NF-κB transcription factor assay using stably transfected HEK293/NF-κB-Luc cells. As shown in Table 2, the hybrid molecule SylA−GlbA strongly inhibited the

Table 2. Syrbactins Inactivate TNF-α-Induced NF-κB Activity

compound	IC_{50} (μM)[a]
SylA−GlbA	2.87 ± 1.32
SylA	6.80 ± 2.00
GlbA	15.46 ± 2.90
TPCK (control 1)	4.2 ± 0.86
BAY-11 (control 2)	2.6 ± 0.12

[a]Dose−response curves based on eight serial dilutions of syrbactin compounds SylA−GlbA, SylA, and GlbA as well as NF-κB inhibitors TPCK and BAY-11 (positive controls) were used to determine the IC_{50} values. Two independent experiments were performed in triplicate assays (n = 6).

TNF-α-stimulated NF-κB activity and was more potent than SylA or GlbA. Of note, the IC_{50} value of SylA−GlbA (2.87 μM) was comparable with those of well-established NF-κB inhibitors TPCK (4.2 μM) and BAY-11 (2.6 μM), which were included as controls. These results demonstrate for the first time that like bortezomib, syrbactin-promoted proteasome blockage results in the inhibition of NF-κB activity, which then leads to apoptosis as we previously demonstrated.[8,24]

Crystal Structure of SylA−GlbA with the Yeast 20S Proteasome. In comparison with the natural product SylA, the synthetic SylA−GlbA analogue revealed significantly decreased IC_{50} values for all three proteolytically active sites of approximately 3 orders of magnitude. Hence, we performed crystal structure analysis of SylA−GlbA in complex with the yeast proteasome at 2.8 Å resolution (R_{free} = 24.4%) for characterizing the ligand at the molecular level in comparison to SylA and GlbA. The electron density map displays the macrolactam ring of the SylA−GlbA ligand covalently bound to the Thr1O$^{\gamma}$ atom by formation of an irreversible ether bond (Figure 4A,B). The oxyanion hole is occupied by the carbonyl oxygen of the reactive 1,4-Michael headgroup of the ligand. The SylA−GlbA peptide moiety adopts the formation of an antiparallel β-sheet in the nonprimed substrate binding channel as observed previously.[44] Furthermore, in the case of the CT-L and T-L active site, the peptide backbone is also stabilized by hydrogen bond formation with Asp114 located on the adjacent subunit being either β6 or β2. Of note, this additional stabilization is absent in the substrate binding channel forming the C-L site and explains the reduced affinity of SylA, GlbA, and SylA−GlbA for the latter. Substantial variations in the binding probability among the CT-L, T-L, and C-L activities are caused by the molecular flexibility of the distinct specificity pockets with respect to entropic and enthalpic ligand stabilization, thus being a prime cause for the preference of the syrbactins to predominantly block the CT-L site.

Interestingly, although the structural superposition of the macrolactom rings of SylA, GlbA, and SylA−GlbA is almost perfect [root-mean-square deviation of <0.2 Å (Figure 4C)], major differences in binding affinity exist among SylA, GlbA, and SylA−GlbA. This discrepancy can be explained as follows.

dx.doi.org/10.1021/bi300841r | Biochemistry 2012, 51, 6880−6888

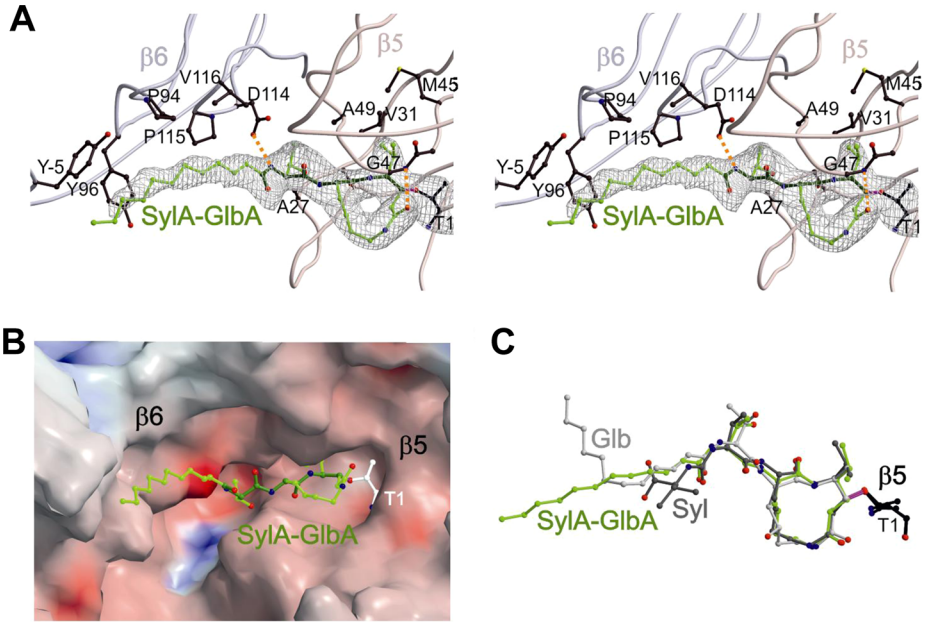

Figure 4. Structural characterization of SylA−GlbA. (A) Stereoview of the $2F_o - F_c$ electron density map (gray mesh, 1σ) for the CT-L substrate binding channel in complex with SylA−GlbA (colored green), which has been omitted from prior phase calculations. The backbones of subunits $\beta5$ and $\beta6$ are presented as rose and gray coils, respectively; side chains involved in ligand stabilization are drawn in a ball-and-stick representation, whereas hydrogen bonds are indicated by orange dashed lines. The lipophilic pocket stabilizing the aliphatic linker of SylA−GlbA is formed by Tyr6, Pro94, Tyr96, and Pro115 from subunit $\beta6$. Note the amino acid numbering of side chain residues is that of Loewe et al.[52] (B) Surface charge distribution for the CT-L active site. Surface colors indicate positive and negative electrostatic potentials contoured from 50 kT/e (intense blue) to −50 kT/e (intense red). Thr1 is colored white and the inhibitor SylA−GlbA highlighted in green as in panel A. (C) Structural superposition of SylA−GlbA (green), GlbA (gray), and SylA (dark gray) bound to the CT-L site. Thr1 of subunit $\beta5$ is colored black. The orientation is that of panel A.

(i) SylA harbors an isopropyl side chain in P4, which, however, because of the presence of a urea moiety between P3 and P4, is out of frame and therefore performs only impaired interactions with the S4 specificity pocket. (ii) The N-terminal aliphatic fatty acid chains in GlbA and SylA−GlbA, which point toward the adjacent subunit $\beta6$ in the CT-L substrate binding channel, becomes stabilized in an apolar pocket (Figure 4A). Remarkably, although the lipophilic tails between GlbA and SylA−GlbA differ in their orientation (Figure 4C), the in vitro IC_{50} values of the natural product and the SylA−GlbA compound are quite similar. Thus, the strong binding affinity of GlbA and SylA−GlbA compared to that of SylA can be explained by the presence of the aliphatic linker that is flexible in solution but is bound to hydrophobic patches of the central hydrolytic proteasomal chamber upon docking of the ligand to the proteolytic center. As a result and in contrast to SylA, this additional stabilization of GlbA as well as SylA−GlbA in the vicinity of the active site increases the mean residence time of the ligands and therefore allows completion of formation of the irreversible ether bond with the Thr1O^{γ} atom.

DISCUSSION

Natural products involved in plant−pathogen interactions can serve as an inspiring source for the identification of new bioactive entities and provide strategies for how to achieve small molecule manipulation of biological systems.[45] Syrbactin is a subordinate term for the syringolin, glidobactin, and cepafungin natural product families, and their grouping is based on their related molecular frameworks, similar biosynthesis pathways, and identical modes of action, irreversible proteasome inhibition.[46] Syrbactins are now recognized as a new and structurally distinct class of proteasome inhibitors,[15] which prompted the design of synthetic syrbactin-inspired analogues.[23−27]

Our study demonstrates that the synthetic hybrid molecule SylA−GlbA is a potent proteasome inhibitor and blocks the three subcatalytic activities in a dose-dependent manner and at concentrations comparable with that of bortezomib. SylA−GlbA also substantially inhibits the proliferation of several cancer cell lines, with most potent effects in multiple myeloma. While proteasome inhibition is a validated strategy for therapy of multiple myeloma, relapse is common and often associated with chemoresistance. Therefore, the identification of novel compounds that overcome resistance to conventional drugs as well as nonspecific proteasome inhibitors is increasingly important.[20] Intriguingly, the dexamethasone-sensitive (MM1.S) and dexamethasone-resistant (MM1.RL) multiple myeloma cell lines were both inhibited by SylA−GlbA in the nanomolar range with IC_{50} values of 28 and 27 nM, respectively, suggesting that SylA−GlbA is equally effective in multiple myeloma cells that exhibit chemoresistance to a conventional drug. In contrast, the (wild-type) SylA was significantly less potent in both multiple myeloma cell lines and cell treatments required ∼5-fold higher drug concentrations in dexamethasone-resistant cells to achieve comparable growth inhibition (8.5 and 39.3 μM, respectively).[24]

The NF-κB transcription factor plays an important role in tumorigenesis through induction of cell proliferation, suppression of apoptosis, metastasis, and induction of angiogenesis.[47] Bortezomib inhibits NF-κB activity, the mechanism attributed to its antitumor actions, which led to its approval by the Food and Drug Administration (FDA) in 2003 for the treatment of multiple myeloma. On the basis of our findings, syrbactins inactivate TNF-α-activated NF-κB in stably transfected

dx.doi.org/10.1021/bi300841r | Biochemistry 2012, 51, 6880−6888

HEK293/NF-κB-Luc cells at micromolar concentrations, with the strongest potency occurring in multiple myeloma.

Given the large number of substrates of the proteasome, it seems surprising that inhibition of NF-κB activity should be the only mechanism by which proteasome inhibitors exert their antitumor effects. Indeed, other proteasome inhibitors, including clasto-lactacystin, do not lead to the accumulation of IκB in the cytoplasm and nuclear loss of NF-κB and therefore do not inhibit NF-κB activity.[48,49] Moreover, a paradigm shift was recently introduced proposing that NF-κB inhibition might be irrelevant to the effects of bortezomib in multiple myeloma cells and involves other signaling routes and proteasome-independent degradation of IκBα.[50,51] The possible activation of distinct and cell-type specific downstream cell signaling events in response to proteasome inhibition might also explain why SylA−GlbA treatments were most effective in multiple myeloma cells (Figure 3), despite the fact that the inhibition of proteasomal activities by SylA−GlbA was similar in all five tested cell lines (Figure 2).

The structural evaluation of SylA, GlbA, and SylA−GlbA suggests an improved binding probability starting from a charged and highly polar moiety adjacent to the macrolactam scaffold in SylA with impaired binding affinity and continuing with an enhanced decoration as well as exploitation of the distant hydrophobic pocket by an aliphatic linker that eventually can further be optimized with maximal inhibition values for future syrbactin derivatives. Thus, the structural elucidation of the SylA−GlbA complex and its comparison with SylA and GlbA facilitate novel innovations via fragment-based drug design strategies for the discovery of new chemical entities as demonstrated by the aliphatic linker of either the natural product GlbA or its synthetic derivative SylA−GlbA.

In summary, we have characterized the novel synthetic syrbactin analogue SylA−GlbA that incorporates unique structural features of both SylA and GlbA, creating a hybrid molecule that exhibits enhanced biological activity versus other syrbactin compounds and is comparable with well-studied proteasome inhibitors such as the FDA-approved bortezomib used in the clinic. It is tempting to speculate that syrbactins could similarly be developed into a drug for the treatment of multiple myeloma and likely other types of cancer. To achieve this, further development of next-generation syrbactin analogues will be important in an endeavor to create other clinically relevant proteasome inhibitors that may be used to achieve therapeutic synergisms or as replacement therapies for bortezomib-chemoresistant multiple myeloma and other forms of cancer.[17]

■ ASSOCIATED CONTENT

Ⓢ Supporting Information

Data collection and refinement statistics for the proteasome:-SylA−GlbA complex structures. This material is available free of charge via the Internet at http://pubs.acs.org.

Accession Codes

Atomic coordinates and the structural factors are deposited in the Protein Data Bank as entry 4GK7.

■ AUTHOR INFORMATION

Corresponding Author

*Department of Pharmaceutical Sciences, College of Pharmacy, University of Hawaii at Hilo, 34 Rainbow Dr., Hilo, HI 96720. Telephone: (808) 933-2807. Fax: (808) 933-2974. E-mail: andre@hawaii.edu.

Present Addresses

#Department of Biochemistry, University of Texas Health Science Center at San Antonio, San Antonio, TX 78229.

●Wellcome Trust Centre for Cell-Matrix Research, Faculty of Life Sciences, University of Manchester, Manchester M13 9PT, U.K.

○Institut für Organische and Biomolekulare Chemie, Universität Göttingen, Tammannstr. 2, 37077 Göttingen, Germany.

Funding

This work was supported by the Robert C. Perry Fund of the Hawaii Community Foundation (HCF Grant 10ADVC-47862, A.S.B.) and the Hawaii Business and Acceleration Mentors (HiBEAM, A.S.B.). Further support was provided by an ERC Starting Grant (ERC Grant Agreement 258413, M.K.), the Swiss National Science Foundation (Grant 31003A-134936, R.D.), and the German-Israeli Foundation for Scientific Research and Development (GIF Grant 1102/2010, M.G.).

Notes

The authors declare no competing financial interest.

■ ACKNOWLEDGMENTS

We are grateful to Prof. Dr. Nancy L. Krett (Northwestern University) for providing multiple myeloma cells (MM1.S, MM1.RL, and U266). Dr. Dana-Lynn Koomoa and Erin Mitsunaga are thanked for initial contributions to this project, and Richard Feicht is thanked for yeast proteasome purification. We acknowledge the staff of beamlines X06SA and X06DA at the Paul Scherrer Institute, SLS, for their support during data collection.

■ REFERENCES

(1) Amrein, H., Makart, S., Granado, J., Shakya, R., Schneider-Pokorny, J., and Dudler, R. (2004) Functional analysis of genes involved in the synthesis of syringolin A by *Pseudomonas syringae* pv. syringae B301 D-R. *Mol. Plant-Microbe Interact. 17*, 90−97.

(2) Oka, M., Nishiyama, Y., Ohta, S., Kamei, H., Konishi, M., Miyaki, T., Oki, T., and Kawaguchi, H. (1988) Glidobactins A, B and C, new antitumor antibiotics. I. Production, isolation, chemical properties and biological activity. *J. Antibiot. 41*, 1331−1337.

(3) Oka, M., Numata, K., Nishiyama, Y., Kamei, H., Konishi, M., Oki, T., and Kawaguchi, H. (1988) Chemical modification of the antitumor antibiotic glidobactin. *J. Antibiot. 41*, 1812−1822.

(4) Oka, M., Ohkuma, H., Kamei, H., Konishi, M., Oki, T., and Kawaguchi, H. (1988) Glidobactins D, E, F, G and H; minor components of the antitumor antibiotic glidobactin. *J. Antibiot. 41*, 1906−1909.

(5) Oka, M., Yaginuma, K., Numata, K., Konishi, M., Oki, T., and Kawaguchi, H. (1988) Glidobactins A, B and C, new antitumor antibiotics. II. Structure elucidation. *J. Antibiot. 41*, 1338−1350.

(6) Wäspi, U., Blanc, C., Winkler, C., Ruedi, P., and Dudler, R. (1998) Syringolin, a novel peptide elicitor from *Pseudomonas syringae* pv. *syringae* that induces resistance to *Pyricularia oryzae* in rice. *Mol. Plant-Microbe Interact. 11*, 727−733.

(7) Wäspi, U., Hassa, P., Staempfli, A. A., Molleyres, L. P., Winker, T., and Dudler, R. (1999) Identification and structure of a family of syringolin variants: Unusual cyclic peptides from *Pseudomonas syringae* pv. *syringae* that elicit defense responses in rice. *Microbiol. Res. 154*, 89−93.

(8) Coleman, C. S., Rocetes, J. P., Park, D. J., Wallick, C. J., Warn-Cramer, B. J., Michel, K., Dudler, R., and Bachmann, A. S. (2006) Syringolin A, a new plant elicitor from the phytopathogenic bacterium *Pseudomonas syringae* pv. *syringae*, inhibits the proliferation of

neuroblastoma and ovarian cancer cells and induces apoptosis. *Cell Proliferation 39*, 599−609.
(9) Groll, M., Schellenberg, B., Bachmann, A. S., Archer, C. R., Huber, R., Powell, T. K., Lindow, S., Kaiser, M., and Dudler, R. (2008) A plant pathogen virulence factor inhibits the eukaryotic proteasome by a novel mechanism. *Nature 452*, 755−758.
(10) Adams, J. (2003) The proteasome: Structure, function, and role in the cell. *Cancer Treat. Rev. 29* (Suppl.1), 3−9.
(11) Chitra, S., Nalini, G., and Rajasekhar, G. (2012) The ubiquitin proteasome system and efficacy of proteasome inhibitors in diseases. *Int. J. Rheum. Dis. 15*, 249−260.
(12) Huber, E. M., and Groll, M. (2012) Inhibitors for the Immuno- and Constitutive Proteasome: Current and Future Trends in Drug Development. *Angew. Chem., Int. Ed.*, DOI: 10.1002/anie.201201616.
(13) Moreau, P., Richardson, P. G., Cavo, M., Orlowski, R. Z., San Miguel, J. F., Palumbo, A., and Harousseau, J. L. (2012) Proteasome inhibitors in multiple myeloma: Ten years later. *Blood 120*, 947−959.
(14) Adams, J. (2004) The proteasome: A suitable antineoplastic target. *Nat. Rev. Cancer 4*, 349−360.
(15) Kisselev, A. F. (2008) Joining the army of proteasome inhibitors. *Chem. Biol. 15*, 419−421.
(16) Kisselev, A. F., and Goldberg, A. L. (2001) Proteasome inhibitors: From research tools to drug candidates. *Chem. Biol. 8*, 739−758.
(17) Orlowski, R. Z., and Kuhn, D. J. (2008) Proteasome inhibitors in cancer therapy: Lessons from the first decade. *Clin. Cancer Res. 14*, 1649−1657.
(18) Rajkumar, S. V., Richardson, P. G., Hideshima, T., and Anderson, K. C. (2005) Proteasome inhibition as a novel therapeutic target in human cancer. *J. Clin. Oncol. 23*, 630−639.
(19) Voorhees, P. M., Dees, E. C., O'Neil, B., and Orlowski, R. Z. (2003) The proteasome as a target for cancer therapy. *Clin. Cancer Res. 9*, 6316−6325.
(20) Kuhn, D. J., Hunsucker, S. A., Chen, Q., Voorhees, P. M., Orlowski, M., and Orlowski, R. Z. (2009) Targeted inhibition of the immunoproteasome is a potent strategy against models of multiple myeloma that overcomes resistance to conventional drugs and nonspecific proteasome inhibitors. *Blood 113*, 4667−4676.
(21) Huber, E. M., Basler, M., Schwab, R., Heinemeyer, W., Kirk, C. J., Groettrup, M., and Groll, M. (2012) Immuno- and constitutive proteasome crystal structures reveal differences in substrate and inhibitor specificity. *Cell 148*, 727−738.
(22) Clerc, J., Groll, M., Illich, D. J., Bachmann, A. S., Huber, R., Schellenberg, B., Dudler, R., and Kaiser, M. (2009) Synthetic and structural studies on syringolin A and B reveal critical determinants of selectivity and potency of proteasome inhibition. *Proc. Natl. Acad. Sci. U.S.A. 106*, 6507−6512.
(23) Anshu, A., Thomas, S., Agarwal, P., Ibarra-Rivera, T. R., Pirrung, M. C., and Schonthal, A. H. (2011) Novel proteasome-inhibitory syrbactin analogs inducing endoplasmic reticulum stress and apoptosis in hematological tumor cell lines. *Biochem. Pharmacol. 82*, 600−609.
(24) Archer, C. R., Koomoa, D. L., Mitsunaga, E. M., Clerc, J., Shimizu, M., Kaiser, M., Schellenberg, B., Dudler, R., and Bachmann, A. S. (2010) Syrbactin class proteasome inhibitor-induced apoptosis and autophagy occurs in association with p53 accumulation and Akt/PKB activation in neuroblastoma. *Biochem. Pharmacol. 80*, 170−178.
(25) Clerc, J., Schellenberg, B., Groll, M., Bachmann, A. S., Huber, R., Dudler, R., and Kaiser, M. (2010) Convergent synthesis and biological evaluation of Syringolin A and derivatives as eukaryotic 20S proteasome inhibitors. *Eur. J. Org. Chem. 21*, 3991−4003.
(26) Ibarra-Rivera, T. R., Opoku-Ansah, J., Ambadi, S., Bachmann, A. S., and Pirrung, M. C. (2011) Syntheses and cytotoxicity of syringolin B-based proteasome inhibitors. *Tetrahedron 67*, 9950−9956.
(27) Opoku-Ansah, J., Ibarra-Rivera, T. R., Pirrung, M. C., and Bachmann, A. S. (2012) Syringolin B-inspired proteasome inhibitor analogue TIR-203 exhibits enhanced biological activity in multiple myeloma and neuroblastoma. *Pharm. Biol. 50*, 25−29.
(28) Clerc, J., Li, N., Krahn, D., Groll, M., Bachmann, A. S., Florea, B. I., Overkleeft, H. S., and Kaiser, M. (2011) The natural product hybrid of Syringolin A and Glidobactin A synergizes proteasome inhibition potency with subsite selectivity. *Chem. Commun. 47*, 385−387.
(29) Clerc, J., Florea, B. I., Kraus, M., Groll, M., Huber, R., Bachmann, A. S., Dudler, R., Driessen, C., Overkleeft, H. S., and Kaiser, M. (2009) Syringolin A selectively labels the 20 S proteasome in murine EL4 and wild-type and bortezomib-adapted leukaemic cell lines. *ChemBioChem 10*, 2638−2643.
(30) Schellenberg, B., Bigler, L., and Dudler, R. (2007) Identification of genes involved in the biosynthesis of the cytotoxic compound glidobactin from a soil bacterium. *Environ. Microbiol. 9*, 1640−1650.
(31) Wäspi, U., Schweizer, P., and Dudler, R. (2001) Syringolin reprograms wheat to undergo hypersensitive cell death in a compatible interaction with powdery mildew. *Plant Cell 13*, 153−161.
(32) Biedler, J. L., Helson, L., and Spengler, B. A. (1973) Morphology and growth, tumorigenicity, and cytogenetics of human neuroblastoma cells in continuous culture. *Cancer Res. 33*, 2643−2652.
(33) Greenstein, S., Krett, N. L., Kurosawa, Y., Ma, C., Chauhan, D., Hideshima, T., Anderson, K. C., and Rosen, S. T. (2003) Characterization of the MM.1 human multiple myeloma (MM) cell lines: A model system to elucidate the characteristics, behavior, and signaling of steroid-sensitive and -resistant MM cells. *Exp. Hematol. 31*, 271−282.
(34) Fogh, J., and Trempe, G. (1975) New human tumor cell lines. In *Human Tumor Cells In Vitro* (Fogh, J., Ed.) p 155, Plenum Press, New York.
(35) Fogh, J., Wright, W. C., and Loveless, J. D. (1977) Absence of HeLa cell contamination in 169 cell lines derived from human tumors. *J. Natl. Cancer Inst. 58*, 209−214.
(36) Kondratyuk, T. P., Park, E. J., Yu, R., van Breemen, R. B., Asolkar, R. N., Murphy, B. T., Fenical, W., and Pezzuto, J. M. (2012) Novel marine phenazines as potential cancer chemopreventive and anti-inflammatory agents. *Mar. Drugs 10*, 451−464.
(37) Groll, M., and Huber, R. (2005) Purification, crystallization and X-ray analysis of the yeast 20S proteasomes. *Methods Enzymol. 398*, 329−336.
(38) Kabsch, W. (1993) Automatic processing of rotation diffraction data from crystals of initially unknown symmetry and cell constants. *J. Appl. Crystallogr. 26*, 795−800.
(39) Brünger, A., Adams, P., Clore, G., DeLano, W., Gros, P., Grosse-Kunstleve, R., Jiang, J., Kuszewski, J., Nilges, M., Pannu, N., Read, R., Rice, L., Simonson, T., and Warren, G. (1998) Crystallography & NMR system: A new software suite for macromolecular structure determination. *Acta Crystallogr. D1*, 905−921.
(40) Brünger, A. (1992) *X-PLOR version 3.1. A system for X-ray crystallography and NMR*, Yale University Press, New Haven, CT.
(41) Turk, D. (1992) Improvement of a programm for molecular graphics and manipulation of electron densities and its application for protein structure determination. Thesis, Technische Universitaet Muenchen, Munich, Germany.
(42) Groll, M., Ditzel, L., Lowe, J., Stock, D., Bochtler, M., Bartunik, H. D., and Huber, R. (1997) Structure of 20S proteasome from yeast at 2.4 Å resolution. *Nature 386*, 463−471.
(43) Brünger, A. T. (1992) Free R value: A novel statistical quantity for assessing the accuracy of crystal structures. *Nature 355*, 472−475.
(44) Groll, M., Huber, R., and Moroder, L. (2009) The persisting challenge of selective and specific proteasome inhibition. *J. Pept. Sci. 15*, 58−66.
(45) Ottmann, C., van der Hoorn, R. A., and Kaiser, M. (2012) The impact of plant-pathogen studies on medicinal drug discovery. *Chem. Soc. Rev. 41*, 3168−3178.
(46) Krahn, D., Ottmann, C., and Kaiser, M. (2011) The chemistry and biology of syringolins, glidobactins and cepafungins (syrbactins). *Nat. Prod. Rep. 28*, 1854−1867.
(47) Orlowski, R. Z., and Baldwin, A. S., Jr. (2002) NF-κB as a therapeutic target in cancer. *Trends Mol. Med. 8*, 385−389.
(48) Kurland, J. F., and Meyn, R. E. (2001) Protease inhibitors restore radiation-induced apoptosis to Bcl-2-expressing lymphoma cells. *Int. J. Cancer 96*, 327−333.

(49) Masdehors, P., Merle-Beral, H., Maloum, K., Omura, S., Magdelenat, H., and Delic, J. (2000) Deregulation of the ubiquitin system and p53 proteolysis modify the apoptotic response in B-CLL lymphocytes. *Blood 96*, 269−274.
(50) Hideshima, T., Ikeda, H., Chauhan, D., Okawa, Y., Raje, N., Podar, K., Mitsiades, C., Munshi, N. C., Richardson, P. G., Carrasco, R. D., and Anderson, K. C. (2009) Bortezomib induces canonical nuclear factor-κB activation in multiple myeloma cells. *Blood 114*, 1046−1052.
(51) McConkey, D. J. (2009) Bortezomib paradigm shift in myeloma. *Blood 114*, 931−932.
(52) Lowe, J., Stock, D., Jap, B., Zwickl, P., Baumeister, W., and Huber, R. (1995) Crystal structure of the 20S proteasome from the archaeon *T. acidophilum* at 3.4 Å resolution. *Science 268*, 533−539.